PASJ: Publ. Astron. Soc. Japan **63**, 45–51, 2011 February 25

Astrometry of Galactic Star-Forming Region ON 2 N with VERA: Estimation of the Galactic Constants

Kazuma ANDO,[1] Takumi NAGAYAMA,[2] Toshihiro OMODAKA,[1] Toshihiro HANDA,[3*] Hiroshi IMAI,[1]
Akiharu NAKAGAWA,[1] Hiroyuki NAKANISHI,[1] Mareki HONMA,[2] Hideyuki KOBAYASHI,[2] and Takeshi MIYAJI[2]
[1]*Graduate School of Science and Engineering, Kagoshima University, 1-21-35 Kôrimoto, Kagoshima, Kagoshima 890-0065*
[2]*Mizusawa VLBI Observatory, National Astronomical Observatory of Japan, 2-21-1 Osawa, Mitaka, Tokyo 181-8588*
[3]*Institute of Astronomy, The University of Tokyo, 2-21-1 Osawa, Mitaka, Tokyo 181-0015*
ando@milkyway.sci.kagoshima-u.ac.jp, takumi.nagayama@nao.ac.jp

(Received 2010 July 30; accepted 2010 December 24)

Abstract

We performed the astrometry of H_2O masers in the Galactic star-forming region Onsala 2 North (ON 2 N) with the VLBI Exploration of Radio Astrometry (VERA). We obtained a trigonometric parallax of 0.261 ± 0.009 mas, corresponding to a heliocentric distance of 3.83 ± 0.13 kpc. ON 2 N is expected to be on the solar circle, because its radial velocity with respect to the local standard of rest (LSR) is nearly zero. By using the present parallax and proper motions of the masers, the galactocentric distance of the Sun and the Galactic rotation velocity at the Sun are found to be $R_0 = 7.80 \pm 0.26$ kpc and $\Theta_0 = 213 \pm 5\,\mathrm{km\,s^{-1}}$, respectively. The ratio of Galactic constants, namely the angular rotation velocity of the LSR, can be determined more precisely, and is found to be $\Omega_0 = \Theta_0/R_0 = 27.3 \pm 0.8\,\mathrm{km\,s^{-1}\,kpc^{-1}}$, which is consistent with recent estimations, but different from $25.9\,\mathrm{km\,s^{-1}\,kpc^{-1}}$ derived from the recommended values of Θ_0 and R_0 by the International Astronomical Union (1985).

Key words: astrometry — Galaxy: fundamental parameters

1. Introduction

The very long baseline interferometry (VLBI) astrometry allows us to directly measure the distance and proper motions of Galactic maser sources. Thus it is one of the most powerful tools for studying the structure of the Milky Way Galaxy. In fact, recent observations with the VLBI Exploration Radio Astrometry (VERA) and the Very Long Baseline Array (VLBA) have succeeded in measuring a kpc-scale distance with accuracy which exceeds 90% (see, e.g., Hachisuka et al. 2006; Xu et al. 2006; Honma et al. 2007).

The galactocentric distance of the Sun, R_0, and the Galactic circular rotation velocity at the Sun, Θ_0, are two fundamental parameters of studying the structure of the Milky Way Galaxy; they are called here the Galactic constants. The rotation curve of the Milky Way Galaxy and all kinematic distances of the sources in the Milky Way Galaxy are derived from these parameters. Since 1985, the International Astronomical Union (IAU) has recommended us to use values of $R_0 = 8.5$ kpc and $\Theta_0 = 220\,\mathrm{km\,s^{-1}}$. However, recent studies have reported that the new values are different from the recommended ones (e.g., Miyamoto & Zhu 1998; Reid et al. 2009a).

The estimation of the Galactic constants however, is, affected by several independent assumptions: the peculiar motion of the source, systematic noncircular motions of both the source and the local standard of rest (LSR) due to the spiral-arm potential, the nonaxisymmetric potential of the Milky Way Galaxy, the warping motion of the galactic disk, and furthermore the motion of the Sun with respect to the LSR. In this paper to simplify the situation we assume that the source moves in a perfect circular orbit on the disk.

The circle with the radius of galactocentric distance R_0 of the Sun is called the solar circle. All sources on the circle are in a circular orbit with the circular velocity Θ_0 of the LSR, provided that the noncircular motion of a source in the galactic disk is negligible. Due to the symmetric geometry, the radial velocity of a source on the circle is observed to be zero with respect to the LSR, and the proper motion of the source depends only on the Galactic rotation velocity, Θ_0, of the LSR. Therefore, we can derive Θ_0 from the measured proper motion of the source on the circle. We can also derive R_0 from the heliocentric distance of the source, since the source, the Sun, and the Galactic center make an isosceles triangle (figure 1). Thus, we can find directly the value of the angular velocity Ω_0 of the LSR from Θ_0/R_0. Traditionally, this value has been derived from the Oort constants A and B on the basis of kinematic analysis of stars in the solar neighborhood (see Miyamoto & Zhu 1998). The value of this ratio is a constraint on the estimation of one Galactic constant from another. Although the Galactic constants, 8.5 kpc and $220\,\mathrm{km\,s^{-1}}$, are recommended by the IAU, at least one of them should be revised, in the case where the ratio is inconsistent with the observed value.

A massive star-forming region, Onsala 2 North (ON 2 N), is located at Galactic coordinates of $(l, b) = (75.^\circ78, 0.^\circ34)$. Its radial velocity, v_{LSR}, with respect to the LSR is estimated to be $0 \pm 1\,\mathrm{km\,s^{-1}}$ in the NH_3 and CS lines (Olmi & Cesaroni 1999; Codella et al. 2010). Lekht et al. (2006) detected the H_2O masers of ON 2 N at the radial velocity range of -12 to $9\,\mathrm{km\,s^{-1}}$, with their peak flux densities of 10^2–10^3 Jy. These H_2O masers are associated with a 7 mm

* Present address: Graduate School of Science and Engineering, Kagoshima University, 1-21-35 Kôrimoto, Kagoshima, Kagoshima 890-0065.

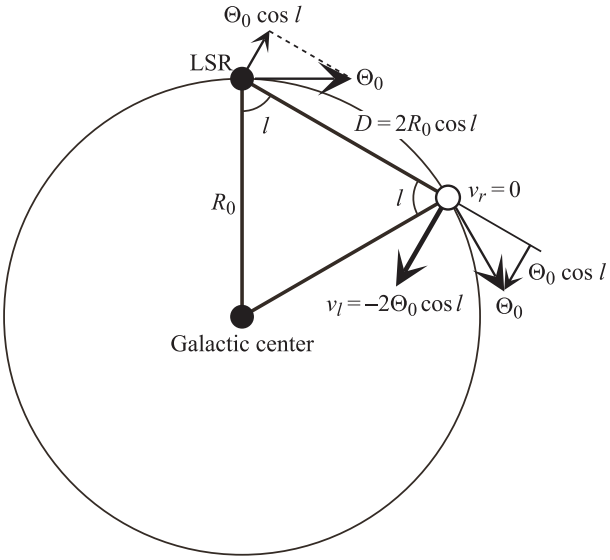

Fig. 1. Method of estimating R_0 and Θ_0 from the distance and the proper motion of the source in the solar circle.

radio continuum source and an NH_3 core as well, which are located at approximately 2″ south from the ultracompact H II region, G75.78+0.34 (Carral et al. 1997; Codella et al. 2010). Thus, ON 2 N is considered to be one of the sources on the solar circle.

We carried out astrometric observations of the H_2O masers in ON 2 N with VERA. Based on these proper motion and trigonometric parallax measurements, we can estimate the Galactic constants Θ_0, R_0, and Ω_0.

In this paper we use the "LSR velocity", or $v_{\rm LSR}$, as the radial velocity with respect to the frame moving toward the solar apex, of which position is approximately $(\alpha,\ \delta)_{1900.0} = (18^{\rm h},\ +30^\circ)$, with $-20\,{\rm km\,s^{-1}}$, namely a provisional solar motion with respect to the LSR to be determined after the traditional definition in radio astronomy since the 1960s (see Kerr & Lynden-Bell 1986).

2. Observations and Data Reductions

We observed H_2O masers at a rest frequency of 22.235080 GHz in the star-forming region ON 2 N with VERA at 14 epochs during the period of $\sim$2 yr. The days of years (DOY) of these epochs are 112, 206, 246, 305, 350 in 2006, 009, 051, 095, 132, 222, 277 in 2007, and 005, 104, 192 in 2008, which are 53847, 53941, 53981, 54040, 54085, 54109, 54151, 54195, 54232, 54322, 54377, 54470, 54569, and 54657 in the Modified Julian Day (MJD) respectively. The data of the first to third epochs were used to estimate the coodinates of H_2O masers. We analyzed the data of the remaining 11 epochs in this study. The H_2O maser source, ON 2 N, and a position-reference-continuum source, ICRF J201528.7+371059 (hereafter J2015+3710) listed in the VLBA Calibrator Survey 2 (VCS2: Fomalon et al. 2003), were simultaneously observed in a dual-beam mode for $\sim$10 hr. The typical on-source integration time was 6 hr for both ON 2 N and J2015+3710. The peak flux density of J2015+3710 was 0.8–2 Jy in each epoch. The two objects, ON 2 N and J2015+3710, are 1.°27 apart. By injecting artifical noise sources into two beams, the instrumental phase difference between the two beams was measured continuously during the observations (Honma et al. 2008a). Left-hand circular polarization signals were filtered with the VERA digital filter unit (Iguchi et al. 2005) and recorded with the VERA DIR2000 recorder system. The data were recorded onto magnetic tapes at a rate of 1024 Mbps, providing a total bandwidth of 256 MHz with 2-bit quantization, which consists of 16 IF channels with a band width of 16 MHz each. One IF channel was assigned to ON 2 N, and the other 15 IF channels were assigned to J2015+3710. The frequency spacing for ON 2 N is 15.625 kHz, corresponding to a velocity spacing of $0.21\,{\rm km\,s^{-1}}$. We carried out the correlation processing using the Mitaka FX correlator.

We used the Astronomical Image Processing System (AIPS) developed by the National Radio Astronomical Observatory (NRAO) for data reduction. An amplitude calibration was performed using the system noise temperatures measured during the observations. For phase-referencing, a fringe fitting was made using the AIPS task FRING on J2015+3710 with a typical integration time of 1 min and a time interval of 30 s. The solutions of the fringe phases, group delays, and delay rates were applied to ON 2 N in order to calibrate the visibility data. Amplitude and phase solutions obtained from the self-calibration of J2015+3710 were also applied to ON 2 N. Visibility phase errors caused by the Earth's atmosphere were calibrated based on GPS measurements of the atmospheric zenith delay, which occurs due to tropospheric water vapor (Honma et al. 2008b). We made spectral-line image cubes, each of which the extent on the sky was 1024 × 1024 pixels with 0.05 mas using the AIPS task IMAGR. The rms noise for each image was approximately 0.1–1 Jy beam^{-1}. A signal-to-noize ratio of 7 was adopted for image detection. The typical size of the synthesized beam was 1.2 mas × 0.9 mas with a position angle of −50°.

3. Results and Discussion

3.1. Overall Properties of H_2O Masers in ON 2 N

Figure 2 shows the scalar-averaged cross-power spectra of H_2O masers in ON 2 N observed with the VERA Mizusawa–Iriki baseline on 2007/051 and 2008/104. Intense emissions with a flux density of ≥ 100 Jy were detected in the LSR velocity range of −5 to $5\,{\rm km\,s^{-1}}$. The center of the velocity range of the intense emissions is close to the LSR velocity of the associated molecular cloud at $v_{\rm LSR} = 0 \pm 1\,{\rm km\,s^{-1}}$ of the NH_3 and CS lines (Olmi & Cesaroni 1999; Codella et al. 2010). The majority of $v_{\rm LSR}$ of H_2O masers are found in the range of $-12 \leq v_{\rm LSR} \leq 9\,{\rm km\,s^{-1}}$, seen in the previous monitoring observations in 1995–2004 (Lekht et al. 2006). We also detected blueshifted components at $v_{\rm LSR} = -33$ and $-17\,{\rm km\,s^{-1}}$ and a redshifted component at $19\,{\rm km\,s^{-1}}$, which were not detected in previous observations (e.g., Lekht et al. 2006).

Thirty H_2O maser spots were detected over a period of half year and at more than three epochs. They were in the LSR velocity range of −33 to $19\,{\rm km\,s^{-1}}$, and distributed

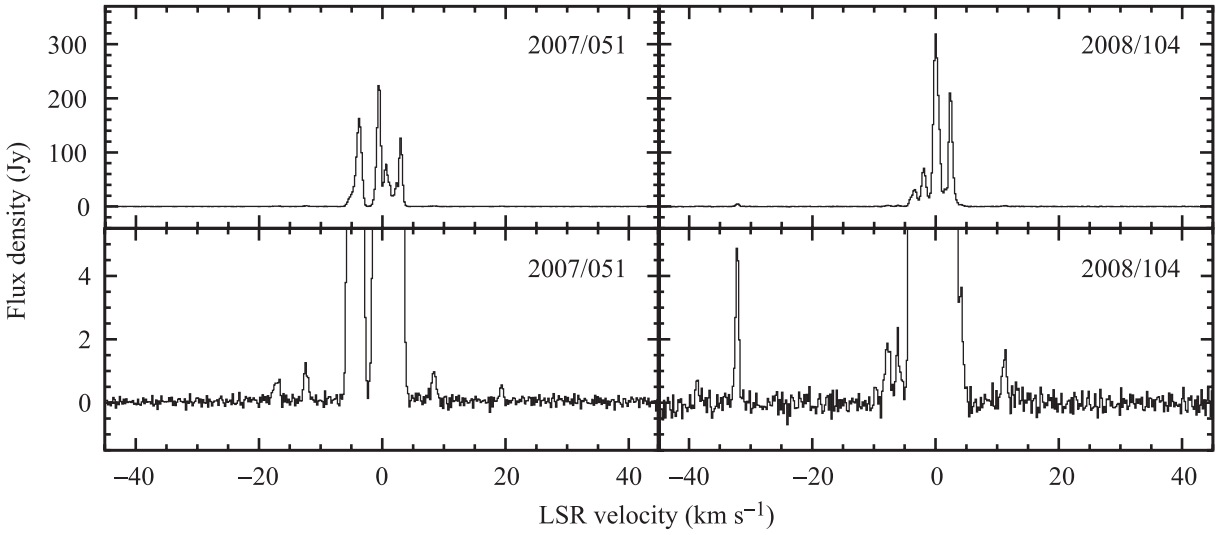

Fig. 2. Scalar-averaged cross-power spectra of H_2O masers in ON 2 N observed with the VERA Mizusawa–Iriki baseline at 2007/051 and 2008/104.

with an area of $1\overset{''}{.}0 \times 0\overset{''}{.}4$. Figure 3 shows the distribution of the internal motion of the maser spots in ON 2 N. The reference position of the map is set at the position of a maser spot at $v_{\rm LSR} = 0.1\,{\rm km\,s^{-1}}$, which is estimated to be $(\alpha, \delta)_{\rm J2000.0} = (20^{\rm h}21^{\rm m}44\overset{\rm s}{.}01225, 37^\circ36'37\overset{''}{.}4844)$. Although the H_2O masers are located at $2''$ south from the peak of the 6 cm radio continuum emission (Wood & Churchwell 1989), they are spatially coincident with the peaks of the 7 mm radio continuum emission and the NH_3 (3, 3) emission (Carral et al. 1997; Codella et al. 2010).

3.2. Parallax and Proper Motion

The absolute motion of the individual H_2O maser spot, i.e., its motion with respect to the position-reference source J2015+3710, is given by the sum of the proper motion and the annual parallactic motion. In order to separate one from the other, we performed monitoring observations of the H_2O masers of ON 2 N for ~ 2 yr.

We made a combined parallax fit, which means a fitting of the positions of 30 H_2O maser spots to a common parallax, but different proper motions and position offsets for individual spots. Figure 4 and table 1 show the results of the combined parallax fit. As can be clearly seen in figure 4, the observed points demonstrate a sinusoidal modulation with a period of 1 yr caused by the annual parallax. For this fitting, we assigned independent "error floors" in quadrature with the formal position-fitting uncertainties. Trial combined fits were conducted and separately reduced χ^2 (per degree of freedom) statistics were applied for the right-ascension and declination residuals. The error floors of 0.088 mas in right ascension and 0.111 mas in declination were then adjusted iteratively so as to achive a reduced χ^2 per degree of freedom near to unity in each coordinate. Combining all of the fittings, we obtained a trigonometric parallax of the H_2O maser spots, 0.261 ± 0.009 mas. The parallax gives a heliocentric distance of ON 2 N, 3.83 ± 0.13 kpc.

In table 1, we also give estimated parallaxes using individual fittings for individual maser spots. We made these individual fittings only for 14 maser spots that were detected over a period of one year. The parallaxes obtained from the individual fittings are consistent with each other and with the result of the combined fit. This means that the parallax obtained by the combined fitting is reliable.

The systemic motion of the source can be estimated to be an average motion of all maser spots, provided that the internal motion is random, or symmetric. We believe that this may be reasonable for ON 2 N because of the following two reasons. The average radial velocity of all maser spots is $-1.2\,{\rm km\,s^{-1}}$, which is close to the systemic one derived from the associated molecular cloud. This suggests that the maser spots move rather symmetrically. Figure 3 shows the residual proper-motion vectors, which are the differences between the individual proper motions and the average. We did not find any strong asymmetric motion. Therefore, we find that the reasonable absolute proper motions are not biased by the internal motions of ON 2 N. Thus, the systemic proper motion of ON 2 N is estimated to be $(\mu_\alpha \cos\delta, \mu_\delta) = (-2.79 \pm 0.13, -4.66 \pm 0.17)\,{\rm mas\,yr^{-1}}$, an average motion of all 30 maser spots.

Using the Galactic coordinates of ON 2 N, $(l, b) = (75\overset{\circ}{.}78, -0\overset{\circ}{.}34)$, we calculate that the proper-motion components in the Galactic coordinates are $(\mu_l \cos b, \mu_b) = (-5.42 \pm 0.16, -0.36 \pm 0.14)\,{\rm mas\,yr^{-1}}$, corresponding to a linear velocity of $(v_l, v_b) = (-98.4 \pm 2.9, -6.6 \pm 2.6)\,{\rm km\,s^{-1}}$ at a distance of 3.83 kpc. We note that these values are still affected by the solar motion, because the observed proper motion is not relative to the LSR, but to the Sun.

To convert this observed velocity to that with respect to the LSR, we have to fix the solar motion relative to the LSR. As mentioned in section 1, we use the solar motion in the traditional definition of $(U_\odot, V_\odot, W_\odot) = (+10.3, +15.3, +7.7)\,{\rm km\,s^{-1}}$ by Reid et al. (2009a).[1] We note that

[1] This velocity is consistent with the provisional solar motion we used, but the 3 dimensional linear velocity $(U_\odot, V_\odot, W_\odot) = (+10.0, +15.4, +7.8)\,{\rm km\,s^{-1}}$ shown in Kerr and Lynden-Bell (1986) is inconsistent with the definition by themselves.

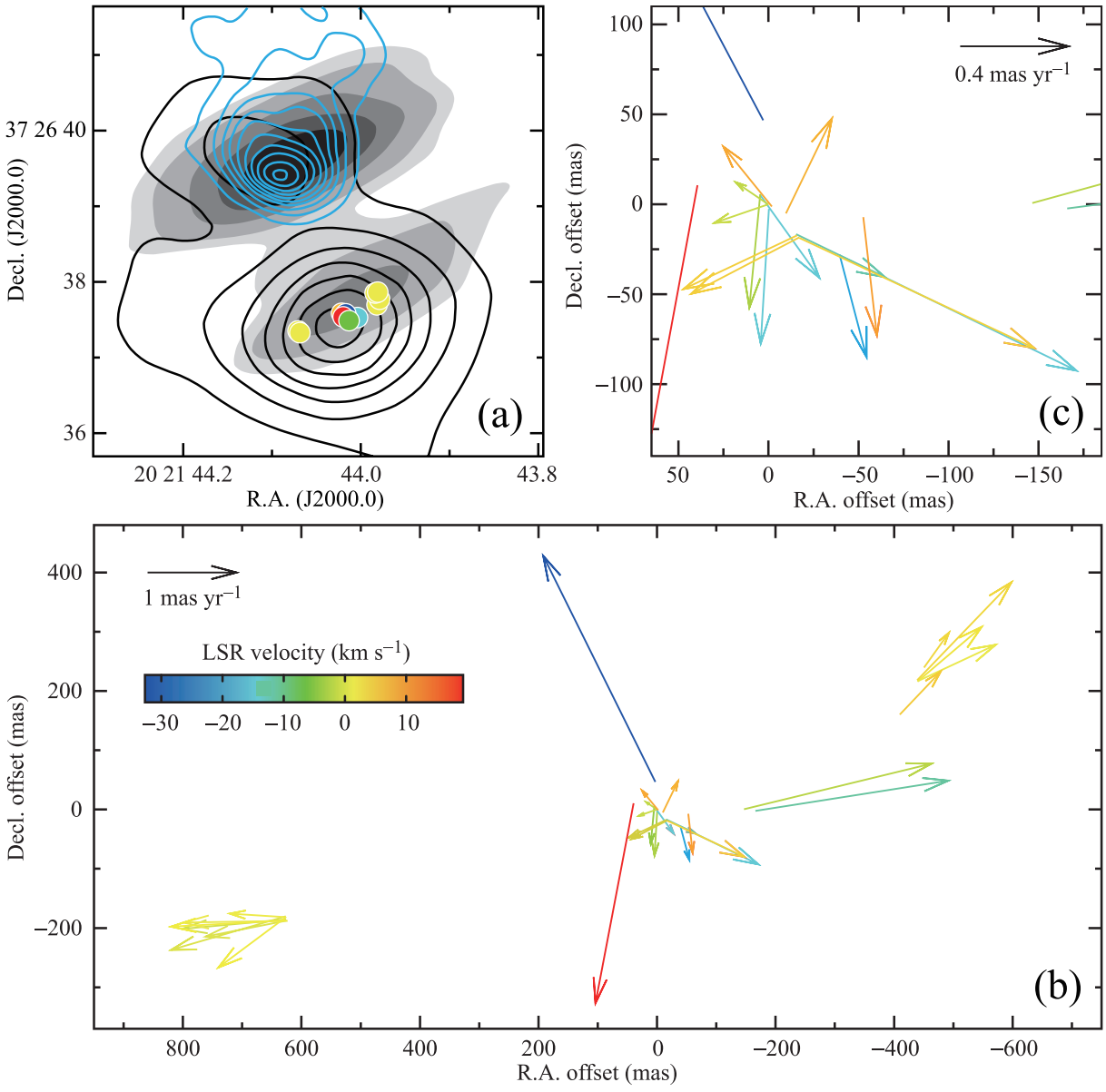

Fig. 3. (a) Distributions of H_2O masers (color filled circles) superimposed on the 6 cm radio continuum emission (cyan contour: Wood & Churchwell 1989), the 7 mm radio continuum emission (gray contour: Carral et al. 1997), and the NH_3 (3,3) emission (black contour: Codella et al. 2010). (b) Internal motion vectors of H_2O masers. The spot color shows the LSR velocity. The arrow at the top-left corner shows an internal motion of 1 mas yr^{-1}, corresponding to 18.2 km s^{-1} at a distance of 3.83 kpc. (c) Close-up to the central part of (b).

this set of values is very close to that found by Miyamoto and Zhu (1998) (see their table 5) on the basis of a stellar motion analysis of the HIPPARCOS proper motions in the solar neighborhood. Using this traditional solar motion, we convert the observed proper motion to $(\mu_l \cos b,\ \mu_b) = (-5.76 \pm 0.16,\ 0.02 \pm 0.14)$ mas yr^{-1}, corresponding to a linear velocity, $(v_l,\ v_b) = (-104.6 \pm 2.9,\ 1.1 \pm 2.6)$ km s^{-1} relative to the LSR.

3.3. *Derivation of the Galactic Constants*

Based on the observed LSR velocity of ON 2 N, we believe that the source is located at, or close to, the solar circle. The small proper motion along the Galactic latitude, $v_b = 1.1 \pm 2.6$ km s^{-1}, described in section 3 supports that ON 2 N moves in a circular orbit around the Galactic center.

For an object on the solar circle, the galactocentric distance of the Sun, or that of the source, R_0, is estimated from the heliocentric distance of the source to be

$$R_0 = \frac{D}{2\cos l}, \tag{1}$$

where l is the Galactic longitude of the source (see figure 1). Our estimation of the heliocentric distance of ON 2 N yields $D = 3.83 \pm 0.13$ kpc. It gives $R_0 = 7.80 \pm 0.26$ kpc, if ON 2 N is exactly located on the solar circle. This value is close to the previous estimations; R_0 is estimated to be 8.0 ± 0.5 kpc

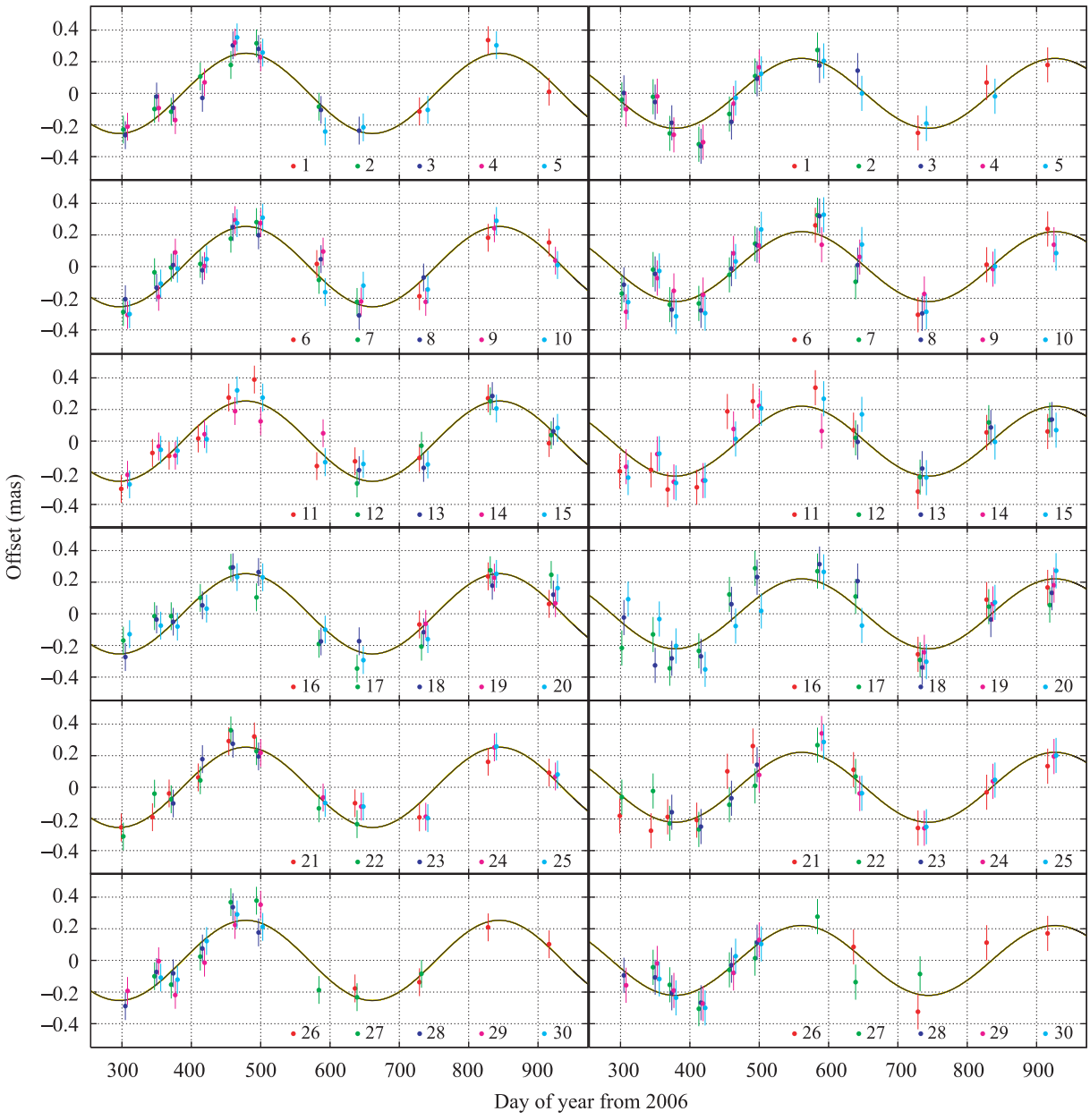

Fig. 4. Parallax of the H_2O masers in ON 2 N. The data for the different maser positions are slightly shifted in time for clarity. Individual proper motions and position offsets are removed. The left and right panels show the annual parallaxes in right ascension and declination, respectively. The numbers in each panel show the ID numbers of the spot listed in table 1.

from a combination of many methods reviewd by Reid (1993), $7.9^{+0.8}_{-0.7}$ kpc from a parallax measurement of H_2O masers in Sgr B2 with the VLBA (Reid et al. 2009b), and 8.28 ± 0.44 kpc using the orbits of stars around Sgr A* from the Very Large Telescope (VLT) and Keck data (Gillessen et al. 2009).

For a source on the solar circle with perfect circular motion, its proper-motion velocity along the Galactic longitude, v_l, gives the galactic rotation velocity of the LSR or that of the object as

$$\Theta_0 = -\frac{v_l}{2\cos l}, \qquad (2)$$

where l is the Galactic longitude of the source. Our measured value of $v_l = -104.6 \pm 2.6\,\mathrm{km\,s^{-1}}$ gives $\Theta_0 = 213 \pm 5\,\mathrm{km\,s^{-1}}$. This value is smaller than that estimated by Reid et al. (2009a), $\Theta_0 = 254 \pm 16\,\mathrm{km\,s^{-1}}$, but close to the IAU recommended value of $\Theta_0 = 220\,\mathrm{km\,s^{-1}}$.

Our derivations of the Galactic constants are strongly dependent on the assumption of the location of ON 2 N in the Milky Way Galaxy. However, we found that the ratio of the Galactic constants, Θ_0/R_0, which is the anglular velocity of the LSR, Ω_0, can be estimated less dependently on the assumption. The value of Θ_0/R_0 can be estimated, even if ON 2 N is not exactly located on the solar circle, but near there.

For a source moving in a circular motion at any position in the galactic disk, its radial and tangential velocities with

Table 1. Obtained values of parallax, π, and proper motions, $\mu_\alpha \cos\delta$ and μ_δ, for H_2O maser features in ON 2 N.*

ID	$v_{\rm LSR}$ (km s^{-1})	$\Delta\alpha\cos\delta$ (mas)	$\Delta\delta$ (mas)	Epochs	π (mas)	$\mu_\alpha\cos\delta$ (mas yr^{-1})	μ_δ (mas yr^{-1})
1	−32.8	3.0	46.7	........IJK	——	-1.53 ± 0.24	-2.12 ± 0.31
2	−17.6	−39.5	−28.1	ABCDEFG....	——	-2.89 ± 0.14	-5.04 ± 0.17
3	−16.5	−39.0	−28.2	ABCDEFGH...	0.252 ± 0.043	-3.67 ± 0.10	-5.09 ± 0.13
4	−12.1	−15.3	−16.7	ABCDEF.....	——	-3.12 ± 0.21	-4.82 ± 0.26
5	−10.4	−165.9	−2.4	....EFGHIJ.	0.258 ± 0.024	-4.96 ± 0.10	-4.32 ± 0.13
6	−4.8	−0.2	−2.6	......G.IJK	——	-2.76 ± 0.12	-5.16 ± 0.16
7	−4.8	4.8	5.5	ABCDEFGH...	0.236 ± 0.036	-3.01 ± 0.10	-4.97 ± 0.13
8	−3.7	4.6	5.4	ABCDEFGHI..	0.257 ± 0.037	-2.75 ± 0.08	-5.08 ± 0.10
9	−1.8	−146.6	0.6	ABCDEFGHIJK	0.229 ± 0.038	-4.90 ± 0.04	-4.15 ± 0.06
10	−1.2	0.2	0.0	ABCDEFGHIJK	0.276 ± 0.031	-2.67 ± 0.05	-4.58 ± 0.06
11	0.1	0.0	0.0	ABCDEFGHIJK	0.287 ± 0.039	-2.59 ± 0.05	-4.73 ± 0.06
12	0.5	626.1	−185.4	.......HIJK	——	-1.62 ± 0.15	-4.77 ± 0.19
13	0.7	625.2	−187.6	.......HIJK	——	-1.88 ± 0.15	-4.84 ± 0.19
14	0.7	626.2	−180.2	ABCDEFG....	——	-1.50 ± 0.14	-5.04 ± 0.17
15	1.4	−439.8	216.2	ABCDEFGHIJK	0.252 ± 0.031	-3.51 ± 0.05	-4.05 ± 0.06
16	1.4	623.2	−187.9	........IJK	——	-1.62 ± 0.24	-4.68 ± 0.30
17	1.6	627.7	−181.7	ABCDEFGHIJK	0.272 ± 0.048	-2.17 ± 0.05	-4.62 ± 0.06
18	1.8	−439.5	216.4	ABCDEFGHIJK	0.275 ± 0.031	-3.67 ± 0.05	-4.25 ± 0.06
19	1.8	625.1	−187.3	........IJK	——	-1.49 ± 0.24	-4.73 ± 0.31
20	1.8	625.8	−181.2	ABCDEFGHIJK	0.250 ± 0.034	-2.03 ± 0.05	-5.23 ± 0.06
21	2.0	−450.5	239.4	ABCDEFG.IJK	0.264 ± 0.038	-3.07 ± 0.05	-4.27 ± 0.06
22	2.0	−439.1	218.2	ABCDEFGH...	0.270 ± 0.043	-3.85 ± 0.10	-3.56 ± 0.13
23	2.2	−17.1	−18.7	..CDEF.....	——	-3.66 ± 0.35	-5.07 ± 0.44
24	2.4	−15.8	−17.4	.....FGHIJK	——	-2.37 ± 0.09	-4.86 ± 0.11
25	2.6	−17.1	−18.4	......GHIJK	——	-2.39 ± 0.11	-4.87 ± 0.15
26	3.3	−409.6	160.2	.......HIJK	——	-3.25 ± 0.15	-4.18 ± 0.19
27	5.8	−9.7	−5.1	.BCDEFGHI..	0.292 ± 0.050	-2.96 ± 0.09	-4.31 ± 0.11
28	8.3	−1.9	−1.2	ABCDEF.....	——	-2.61 ± 0.20	-4.44 ± 0.26
29	8.7	−52.7	−7.2	ABCDEF.....	——	-2.84 ± 0.21	-5.10 ± 0.25
30	19.3	39.5	10.6	.BCDEF.....	——	-2.36 ± 0.27	-6.91 ± 0.34
		Combined fit			0.261 ± 0.009		
		Average				-2.79 ± 0.13	-4.66 ± 0.17

* Columns (3), (4): Right ascension and declination offsets relative to the positon of the maser spot at $v_{\rm LSR} = 0.1\,{\rm km\,s^{-1}}$, and $(\alpha, \delta)_{\rm J2000.0} = (20^{\rm h}21^{\rm m}44\overset{\rm s}{.}01225, 37^\circ 36' 37\overset{''}{.}4844)$.
Column (5): Each alphabetical letter represents the epoch with maser detection. A, B, C, ..., and K mean the 11 epochs from 54040, 54085, ..., and 54657 in MJD, respectively. A dot represents the epoch without detection.
Column (6): Parallax estimated from the individual fitting.
Columns (7), (8): Motions on the sky in the directions along the right ascension and declination.

respect to the LSR can be written as

$$v_r = \left(\frac{\Theta}{R} - \frac{\Theta_0}{R_0}\right) R_0 \sin l, \tag{3}$$

$$v_l = \left(\frac{\Theta}{R} - \frac{\Theta_0}{R_0}\right) R_0 \cos l - \frac{\Theta}{R} D, \tag{4}$$

where R is the actual galactocentric distance of the source, D the heliocentric distance of the source, and Θ the galactic rotation velocity of the source. Equations (3) and (4) yield

$$\begin{aligned}\frac{\Theta_0}{R_0} &= -\frac{v_l}{D} + v_r \left(\frac{1}{D\tan l} - \frac{1}{R_0 \sin l}\right) \\ &= -a_0 \mu_l + v_r \left(\frac{1}{D\tan l} - \frac{1}{R_0 \sin l}\right),\end{aligned} \tag{5}$$

where a_0 is the conversion constant of the unit from angular velocity to linear and its value $4.74\,{\rm km\,s^{-1}\,mas^{-1}\,yr\,kpc^{-1}}$. For a source near the solar circle, its v_r is nearly zero. In this case, equation (5) yields

$$\frac{\Theta_0}{R_0} \simeq -a_0 \mu_l, \tag{6}$$

which is free from R_0. Actually, we found that Θ_0/R_0 is a nearly constant at $6 \leq R_0 \leq 10\,{\rm kpc}$, and a ratio of $\Theta_0/R_0 = 27.3 \pm 0.8\,{\rm km\,s^{-1}\,kpc^{-1}}$ is obtained using $D = 3.83 \pm 0.13\,{\rm kpc}$, $\mu_l = -5.76 \pm 0.16\,{\rm mas\,yr^{-1}}$, and $v_r = 0 \pm 1\,{\rm km\,s^{-1}}$. This value is close to the value of $\Theta_0/R_0 = 28.7 \pm 1.3\,{\rm km\,s^{-1}\,kpc^{-1}}$ obtained from a tangent point source, ON 1 (Nagayama et al. 2011), and to that of $\Theta_0/R_0 = 28.6 \pm 0.2\,{\rm km\,s^{-1}\,kpc^{-1}}$ obtained from a proper-motion measurement of Sgr A* (Reid & Brunthaler 2004), which was revised using the traditional definition of the solar motion by us. However, this value

is inconsistent with that derived from the IAU recommended values of $220\,\mathrm{km\,s^{-1}}/8.5\,\mathrm{kpc} = 25.9\,\mathrm{km\,s^{-1}\,kpc^{-1}}$. This estimation gives another constraint on the Galactic constants, which is independent of the Oort constants derived from the stellar motion near the Sun.

We thank the referee, Dr. Masanori Miyamoto, for his invaluable comments and suggestions. We also thank the staff members of all VERA stations for their assistances in the observations.

References

Carral, P., Kurtz, S. E., Rodríguez, L. F., De Pree, C., & Hofner, P. 1997, ApJ, 486, L103
Codella, C., Cesaroni, R., López-Sepulcre, A., Beltrán, M. T., Furuya, R., & Testi, L. 2010, A&A, 510, A86
Fomalont, E. B., Petrov, L., MacMillan, D. S., Gordon, D., & Ma, C. 2003, AJ, 126, 2562
Gillessen, S., Eisenhauer, F., Fritz, T. K., Bartko, H., Dodds-Eden, K., Pfuhl, O., Ott, T., & Genzel, R. 2009, ApJ, 707, L114
Hachisuka, K., et al. 2006, ApJ, 645, 337
Kerr, F. J., & Lynden-Bell, D. 1986, MNRAS, 221, 1023
Honma, M., et al. 2007, PASJ, 59, 889
Honma, M., et al. 2008a, PASJ, 60, 935
Honma, M., Tamura Y., & Reid M. J. 2008b, PASJ, 60, 951
Iguchi, S., Kurayama, T., Kawaguchi, N., & Kawakami, K. 2005, PASJ, 57, 259
Lekht, E. E., Trinidad, M. A., Mendoza-Torres, J. E., Rudnitskij, G. M., & Tolmachev, A. M. 2006, A&A, 456, 145
Miyamoto, M., & Zhu, Z. 1998, AJ, 115, 1483
Nagayama, T., Omodaka, T., Nakagawa, A., Handa, T., Honma, M., Kobayashi, H., & Kawaguchi, N. 2011, PASJ, 63, 23
Olmi, L., & Cesaroni, R. 1999, A&A, 352, 266
Reid, M. J. 1993, ARA&A, 31, 345
Reid, M. J., et al. 2009a, ApJ, 700, 137
Reid, M. J., & Brunthaler, A. 2004, ApJ, 616, 872
Reid, M. J., Menten, K. M., Zheng, X. W., Brunthaler, A., & Xu, Y. 2009b, ApJ, 705, 1548
Wood, D. O. S., & Churchwell, E. 1989, ApJS, 69, 831
Xu, Y., Reid, M. J., Zheng, X. W., & Menten, K. M. 2006, Science, 311, 54